Contribution of Pacific wind stress to multi-decadal variations in upper-ocean heat content and sea level in the tropical south Indian Ocean

Franziska U. Schwarzkopf and Claus W. Böning

Leibniz-Institut für Meereswissenschaften, Düsternbrooker Weg 20, 24105 Kiel, Germany

Corresponding Author: (fschwarzkopf@ifm-geomar.de)

Abstract

Reconstructions of the spatial pattern of recent multi-decadal sea level trends in the Indian Ocean (IO) indicate a zonally-extended band in the southern tropics where sea level has substantially fallen between the 1960s and 1990s; the decline is consistent with the observed subsurface cooling associated with a shoaling thermocline in this region. Here the origin and spatio-temporal characteristics of these trends are elucidated by a sequence of ocean model simulations. Whereas interannual variability in the southwestern tropical IO appears mainly governed by IO atmospheric forcing, longer term changes in the south tropical IO involve a strong contribution from the western Pacific via wave transmission of thermocline anomalies through the Indonesian Archipelago, and their subsequent westward propagation by baroclinic Rossby waves. The late 20th-century IO subsurface cooling trend reversed in the 1990s, reflecting the major regime shift in the tropical Pacific easterlies associated with the Pacific Decadal Oscillation.

1. Introduction

The global ocean is warming, and sea level is rising, in response to anthropogenic changes in surface heating [*Domingues et al.,* 2008]. Trends in upper ocean heat content during the past 50 years are, however, spatially highly inhomogeneous, reflecting strong effects of oceanic heat redistribution due to changes in ocean circulation [*Doney et al*., 2007]. A prominent large-scale pattern of subsurface cooling from 1960 to 1999 around depths of 100-200 m has been observed in the tropical IO, associated with a shoaling of isopycnals along the thermocline ridge around 10°S [*Han et al*, 2006; *Alory et al.*, 2007]. Corresponding to the decrease in heat content in this zonal band, recent studies of ocean reanalysis products have identified a distinct pattern of multi-decadal sea level decrease during the late 20th century [*Han et al.*, 2010; *Timmermann et al.*, 2010].

Understanding the causes of theses regional trend patterns is of crucial importance for projections of future ocean and climate conditions. The inhomogeneous changes in IO upper ocean heat content and the associated spatial modulation in tropical sea surface warming [*Trenary and Han*, 2008; *Alory and Meyers*, 2009] are likely to influence natural modes of variability and to affect regional climate conditions in IO-rim countries [*Ummenhofer et al.*, 2009; *England et al.*, 2006]. The corresponding sea level decrease in the south tropical IO more than offset the effect of global anthropogenic sea level rise during the last decades; however, projections of future trends, extremely important for various low-lying tropical islands and coastal areas are controversial, ranging from “little or no rise” [*Han et al.*, 2010] to an acceleration of the global mean rise in this area [*Timmermann et al.*, 2010].

Several mechanisms have been invoked to explain the subsurface cooling in the south tropical IO. Simulations with idealized 2-layer models [*Han et al.*, 2006] and an ocean general circulation model [*Trenary and Han*, 2008] attributed the shoaling of the thermocline to anomalous upward Ekman pumping velocities driven by wind stress changes over the IO. In contrast, *Alory et al.* [2007] proposed an oceanic teleconnection between the tropical Pacific

and Indian Oceans via wave processes through the Indonesian Archipelago: noting that the IO cooling trend occurred along the off-equatorial Rossby wave pathway in the latitude range of the Indonesian Throughflow (ITF), they suggested an association with the observed multi-decadal weakening of the Pacific trade winds in the late twentieth century [*Vecchi et al.*, 2006], through a shoaling of the thermocline in the western tropical Pacific [*Williams and Grottoli*, 2010] and a weakening of the ITF [*Wainwright et al.* 2008]. The significance of this oceanic teleconnection for decadal variability in the eastern subtropical IO has been documented in studies of the century-long sea level record at Fremantle, Western Australia [*Feng et al.*, 2004]. For the trends in the interior tropical IO, some indications for a Pacific contribution had been noted in earlier ocean models [*Reason et al.* 1996] and in 20th century climate model experiments [*Cai et al.*, 2008], but its significance and spatio-temporal manifestation are much less clear. In this study the relative contribution of local (IO) vs. remote (Pacific) atmospheric forcing to the (multi-)decadal changes in the tropical IO heat content and sea level is investigated by a sequence of experiments with a global ocean general circulation model.

2. Model Experiments

The simulations build on various global implementations of the ocean/sea-ice numerical NEMO framework [*Madec*, 2008], developed in the European DRAKKAR collaboration [*Barnier et al.*, 2007]. The basic experiment (REF) is a 0.5°-grid hindcast simulation of the ocean's response to atmospheric forcing in 1958-2004 (preceded by a 20-year spin-up), given by the formulations and refined atmospheric reanalysis products developed by *Large and Yeager* [2004] that represent the basis of the Co-ordinated Ocean Reference Experiments (COREs) proposed by *Griffies et al.* [2009]. A companion eddy-permitting version (REF025, using a 0.25°-grid) showed relatively minor effects of model resolution on the evolution of

heat content and sea level in the Indo-Pacific. Results from REF025 are therefore deferred to the supplementary material.

The identification of the causes of IO decadal variability is aided by two experiments with artificial perturbations in the forcing (Fig. S5). In PAC, the world ocean is subject to climatological, 'normal year' forcing, except for the Pacific north of 50°S, where the same interannual forcing is used as in REF. In IND, interannual forcing is applied only to the IO north of 25°S. In order to separate atmospherically-forced ocean variability from spurious model drift, REF was complemented by a simulation (CLIM) over the same time span with climatological forcing everywhere; the trend of this experiment was subtracted from the interannually-forced cases prior to further analysis. For calculation of model sea surface height (SSH) fields, we followed previous studies [e.g., *Wunsch et al.*, 2007] and subtracted the time-varying global-mean SSH; the adjusted fields thus represent regional SSH anomalies due to ocean dynamics.

3. Interannual variability and multi-decadal trend of sea level and heat content

A manifestation of upper ocean heat content variability in the tropical Indo-Pacific is given by the patterns of sea level change provided by satellite altimetry data since 1993 [*Cazenave and Nerem*, 2004]. During the second half of the 1990s, the southwestern Pacific and eastern IO exhibited the strongest sea level rise in the world ocean (Fig. 1). The hindcast simulation REF (Fig. 1a) reproduces the spatial pattern of the observed trend during this period (Fig. S1a); it also captures the large-scale reversal in the decadal tendencies near the end of the 20th century noted by *Lee and McPhaden* [2008]. Time series of SSH anomalies follow the altimeter records (Figs.1c,d,e) and emphasize the close correspondence between regional sea level and upper ocean heat content variability; they also reproduce the long term tide gauge record at Fremantle [cf., *Feng et al.*, 2004] (Fig. 1f).

Although regional sea level is dominated by strong interannual-decadal variability (in some areas exceeding 10 cm in a few years) related to El Niño/Southern Oscillation (ENSO) [e.g. *Behera and Yamagata*, 2010], the model simulation also suggests a pronounced, basin-scale pattern of change on multi-decadal time scales (Fig. 1b): sea level rose during 1960-1999 by 2-3 cm/decade in the subtropical South Pacific and by 1-2 cm/decade in the subtropical South IO; it fell in the western tropical Pacific (by up to 8cm/decade), off western Australia and in the tropical IO, with the strongest decline in the IO occurring along ~10°S (2-3 cm/decade). The spatial pattern and magnitude of the simulated trend in the tropical IO compare well with recent ocean reanalyses [*Timmermann et al.*, 2010; *Han et al.*, 2010]. As discussed in these studies (and shown in Fig. 1c,d,e), these sea level trends are associated with upper ocean warming (cooling) trends related to a deepening (shoaling) of the thermocline.

4. Causes of sub-surface cooling in the south tropical Indian Ocean

The vertical structure of heating and cooling in the IO (Fig. 2) can be compared with the linear trend of zonally-averaged temperature obtained from historical temperature profiles [cf., *Alory et al.*, 2007]. The overall pattern in REF (Fig. 2a) matches the observed trend: a general surface warming, a wedge of deep warming penetrating to ~800 m near 40°S-45°S, and a prominent subsurface cooling trend in the tropical thermocline, with strongest magnitude between 100 m and 300 m near 7°-15°S. As in the observational analysis, the subsurface signals can be accounted for by a shift of isopycnals (Fig. S2a,b): the deep warming to a southward expansion of the subtropical gyre and the tropical cooling to a shoaling of the thermocline.

The role of local atmospheric forcing (in the IO basin) versus remote forcing (in the Pacific) is addressed by the perturbation experiments PAC and IND (Figs. 2b,c). Whereas the surface warming is almost exclusively due to the local forcing, a significant part of the subsurface IO cooling was contributed by the Pacific (wind) forcing (Figs. 2b,e). The

strongest cooling trend in PAC is found in the Indonesian Archipelago and off western Australia, from where a wedge with decreasing values extends west along the tropical south IO. While the remote forcing had a cooling effect all over the IO, the local forcing (Fig. 2c,f) produced an alternating pattern of zonally-extended bands of warming and cooling in the IO thermocline; its contribution to the thermocline cooling was mainly confined to the western basin.

The local and remote contributions to the tropical IO trend are elucidated by time series of heat content anomalies (Fig. 3). The net changes (as simulated in REF) can be understood as a linear superposition of the IO and Pacific forcing effects, i.e., by the sum of the changes simulated in IND and PAC (see Fig. S4). Averaged over the whole zonal extent of the IO (Fig. 3a), the linear trend between 7° and 15°S for 1960-1999 is 0.29 °C/decade in REF, with a larger contribution from PAC (0.18 °C/decade) than from IND (0.10 °C/decade). The changes in the western basin (Fig. 3b) are governed by stronger interannual variability, primarily due to IO forcing, with the multi-decadal trend as a relatively small residual; in contrast, the eastern basin is predominantly under the influence of the remote forcing (Fig. 3c), contributing the bulk (~75%) of the longer-term cooling. On decadal timescales (85-months filtered time series) the correlation between heat content anomalies in REF and PAC is 0.95 for the eastern box. The time series (especially in the eastern basin) indicate that the trend was not monotonous: the cooling began in the mid-1970s after a phase of decadal warming, and it ended in the 1990s (the latter termination standing out especially in PAC).

The spatio-temporal characteristics of the two forcing mechanisms are elucidated further by Hovmoeller diagrams (Fig. 4) that allow an inspection of the connectivity of the heat content changes along the IO thermocline ridge with the variability in the tropical Pacific. In each of the experiments, the heat content variability appears as a manifestation of a Rossby wave signal: westward propagation of the anomalies in the IO latitude band is ~13 cm/s, much higher than the mean speed of the South Equatorial Current (2-3 cm/s) in this area (see Fig.

S3). A similar westward progression is seen for the multi-decadal cooling trend during the 1970s to 1990s. Overall, the set of experiments suggests that both the interannual variability and the multi-decadal changes in the eastern portion of the tropical IO thermocline were predominantly caused by oceanic signals entering from the Pacific (Fig. 4b), whereas the western basin (west of the Ninety-East-Ridge) was more strongly dominated by locally-forced interannual variability (Fig. 4c); local and remote trend contributions there were of comparable magnitude.

5. Concluding discussion

The ocean hindcast simulation based on the CORE atmospheric forcing formulation is shown to capture the late 20th-century subsurface cooling in the south tropical IO [*Han et al.*, 2006; *Alory et al.*, 2007] and its manifestation in sea level [*Han et al.*, 2010; *Timmermann et al.*, 2010]. Aided by experiments with perturbations in the atmospheric forcing the simulations suggest:

- The subsurface cooling and sea level fall occurred mainly between the mid-1970s and mid-1990s, bracketed by opposite tendencies before and after this period: an evolution consistent with the observed long-term sea level changes off western Australia and their interpretation as a footprint of multi-decadal climate variability in the tropical Pacific [*Feng, et al.*, 2004, 2011].
- Both IO and Pacific wind forcing contributed to the tropical IO changes: the IO forcing is the main cause of interannual variability in the western basin, whereas a large fraction of the multi-decadal variations is related to the winds over the Pacific Ocean.
- The multi-decadal Pacific signal progresses westward in the IO with the same speed as the interannual (i.e., ENSO related) variability leaking in from the western tropical

The results have implications for the future evolution of the IO thermocline structure and sea level: in particular, a continuation of the late 20th-century trends could be expected, if the observed weakening of the Pacific trades [*Vecchi et al.*, 2006] and shoaling of the western equatorial Pacific thermocline [*Williams and Grottoli*, 2010] should continue in the 21st century as suggested by anthropogenic climate change simulations [*Collins et al.*, 2010].

Acknowledgements

This work was supported by the DFG through SFB754 (www.sfb754.de). The ORCA05 and ORCA025 coupled ocean/sea-ice model configurations have been developed by the European DRAKKAR collaboration; we acknowledge the contributions of Arne Biastoch to the model integrations. The study benefitted from discussions with Caroline C. Ummenhofer and Ming Feng. We acknowledge computing resources provided by the computing center of Kiel University and the North-German Supercomputing Alliance (HLRN) in Berlin and Hannover. Satellite data are produced by Ssalto/Ducas and distributed by Aviso with support from CNES. Sea level observations at Fremantle are provided by the Permanent Service for Mean Sea Level (PSMSL).

References

Alory, G., S. Wijffels, and G. Meyers (2007), Observed temperature trends in the Indian Ocean over 1960–1999 and associated mechanisms, *Geophys. Res. Lett.*, 34, L02606, doi:10.1029/2006GL028044.

Alory, G. and G. Meyers (2009), Warming of the upper equatorial Indian Ocean and change in the heat budget (1960-99), *J. Clim.*, 22, 93-113, doi:10.1175/2008JCLI2330.1.

Barnier, B. et al.(2007), Eddy-permitting ocean circulation hindcasts of past decades, *CLIVAR Exchanges*, 12(3), 8-10.

Behera, S., and T Yamagata (2010), Imprint of the El Niño Modoki on decadal sea level changes, *Geophys. Res. Lett.*, 37, L23702, doi:10.1029/2010GL045936.

Cai, W., G. Meyers, and G. Shi (2005), Transmission of ENSO signal to the Indian Ocean, *Geophys. Res. Lett.*, 32, L05616, doi:10.1029/2004GL021736.

Cai, W., A. Sullivan, and T. Cowan (2008), Shoaling of the off-equatorial south Indian Ocean thermocline: Is it driven by anthropogenic forcing?, *Geophys. Res. Lett.*, 35, L12711, doi:10.1029/2008GL034174.

Cazenave, A., and R. S. Nerem (2004), Present-day sea level change: observations and causes, *Rev. Geophys.*, 42, RG3001, doi:10.1029/2003RG000139.

Collins, M., S.-I. An, W. Cai, A. Ganachaud, E. Guilyardi, F.-F. Jin, M. Jochum, M. Lengaigne, S. Power, A. Timmermann, G. Vecchi, and A. Wittenberg (2010), The impact of global warming on the tropical Pacific Ocean and El Niño, *Nature Geosci.*, 3, 391-397, doi:10.1038/ngeo868.

Domingues, C. M., J. A. Church, N. J. White, P. J. Gleckler, S. E. Wijffels, P. M. Barker, and J. R. Dunn (2008), Improved estimates of upper-ocean warming and multi-decadal sea-level rise, *Nature*, 453, 1090-1093, doi:10.1038/nature07080.

Doney, S. C., S. Yeager, G. Danabasoglu, W. G. Large, and J. C. McWilliams (2007), Mechanisms governing interannual variability of upper-ocean temperature in a global ocean hindcast simulation, *J. Phys. Oceanogr.*, 37, 1918-1938, doi:10.1175/JPO3089.1.

England, M. H., C.C. Ummenhofer, and A. Santoso (2006), Interannual rainfall extremes over southwest western Australia linked to Indian Ocean climate variability, *J. Clim.*, 19, 1948-1969.

Feng, M., Y. Li, and G. Meyers (2004), Multidecadal variations of Fremantle sea level: footprint of climate variability in the tropical Pacific, *Geophys. Res. Lett.*, 31, L16302, doi:10.1029/2004GL019947.

Feng, M., C.W. Böning, A. Biastoch, E. Behrens, E. Weller, Y. Masumoto (2011), The reversal of the multi-decadal trends of the equatorial Pacific easterly winds, and the Indonesian Throughflow and Leeuwin Current transports, *Geophys. Res. Lett.*, in press.

Griffies, S. M. et al. (2009), Coordinated Ocean-ice Reference Experiments (COREs), *Ocean Model.*, 26, 1-46, doi:10.1016/j.ocemod.2008.08.2007.

Han, W., G. A. Meehl, and A. Hu (2006), Interpretation of tropical thermocline cooling in the Indian and Pacific oceans during recent decades, *Geophys. Res. Lett.*, 33, L23615, doi:10.1029/2006GL027982.

Han, W., G. A. Meehl, B. Rajagopalan, J. T. Fasullo, A. Hu, J. Lin, W. G. Large, J.-W. Wang, X.-W. Quan, L. L. Trenary, A. Wallcraft, T. Shinoda, and S. Yeager (2010), Patterns of Indian Ocean sea-level change in a warming climate, *Nature Geosci.*, 3, 546-550, doi:10.1038/ngeo901.

Large, W.G., and S. G. Yeager (2004), Diurnal to decadal global forcing for ocean and sea-ice models: the data sets and flux climatologies, *NCAR Technical Note,* NCAR/TN-460+STR NCAR.

Lee, T., and M. J. McPhaden (2008), Decadal phase changes in large-scale sea level and winds in the Indo-Pacific region at the end of the 20th century, *Geophys. Res, Lett, 35, L01605, doi:10.1029/2007GL032419.*

Madec, G. (2008), NEMO ocean engine - version 3.1, *Note du Pôle de modélisation de l'Institut Pierre-Simon Laplace No 27*.

Meyers, G. (1996), Variation of Indonesian throughflow and the El Niño - Southern Oscillation, *J. Geophys. Res.*, 101(C5), 12255-12263.

Reason, C. J. C., R. J. Allan, and J. A. Lindesay (1996), Evidence for the influence of remote forcing on interdecadal variability in the southern Indian Ocean, *J. Geophys. Res.*, 101(C5), 11867-11882.

Timmermann, A., S. McGregor, and F.-F. Jin (2010), Wind effects on past and future regional sea level trends in the southern Indo-Pacific, *J. Clim.*, 23, 4429-4437, doi:10.1175/2010JCLI3519.1.

Trenary, L. L., and W. Han (2008), Causes of decadal subsurface cooling in the tropical Indian Ocean during 1961–2000, *Geophys. Res. Lett.*, 35, L17602, doi:10.1029/2008GL034687.

Ummenhofer, C. C., A. Sen Gupta, M. H. England, and C. J. C. Reason (2009), Contributions of Indian Ocean sea surface temperatures to enhanced east African rainfall, *J. Clim.*, 22, 993-1013, doi:10.1175/2008JCLI2493.1.

Vecchi, G. A., B. J. Soden, A. T. Wittenberg, I. M. Held, A. Leetmaa, and M. J. Harrison (2006), Weakening of tropical Pacific atmospheric circulation due to anthropogenic forcing, *Nature*, 44, 73-76, doi:10.1038/natur04744.

Wainwright, L. G., Meyers, S. Wijffels, and L. Pigot (2008), Change in the Indonesian Throughflow with the cliamtic shift of 1976/1977, *Geophys. Res. Lett.*, 35, L03604, doi:10.1029/2007GL031911.

Wijffels, S., and G. Meyers (2004), An intersection of oceanic waveguides: variability in the Indonesian Throughflow region, *J. Phys. Oceanogr.*, 34, 1232-1253.

Williams, B., and A. G. Grottoli (2010), Recent shoaling of the nutricline and thermocline in the western topical Pacific, Geophys. Res. Lett., 37, L22601, doi:10.1029/2010GL044867.

Wunsch, C., R. M. Ponte, and P. Heimbach (2007), Decadal trends in sea level patterns: 1993-2004, *J. Clim.*, 20, 5889-5911, doi:10.1175/2007JCLI1840.1.

Figure Captions

Fig. 1: Linear trend in SSH derived from REF in (cm/yr) for (a) 1993-2001, (b) 1960-1999. Time series for boxes I (c), II (d) and III (e) of SSH anomalies (cm): REF (black), satellite altimetry (cyan); compared to 100-300m heat content anomalies (GJ/m²) (red). Correlations between REF and altimetry are 0.94, 0.94 and 0.91 in box I, II and III. (f) Sea level anomalies at Fremantle: observed (cyan), REF (black); thin lines annual mean, thick lines low-pass (19-years) filtered values; correlations between REF and tide-gauge are 0.89 (0.98) for annual mean (filtered) time series.

Fig. 2: Linear trends (1960-1999) of IO zonal mean temperature (in K/century) for a) REF, b) PAC and c) IND; and of 100-300 m heat content (in PW/m²) for d) REF, e) PAC and f) IND.

Fig. 3: Relative influence of Indian and Pacific forcing on IO changes: heat content anomaly (100-300 m) (GJ/m²) averaged over the boxes marked in Fig. 2 for (a) whole IO extent, b) western IO and c) eastern IO; d) sea level anomaly (cm) at Fremantle for REF (red), PAC (blue), IND (green).

Fig. 4: Zonal propagation of heat content (100-300 m) anomalies (GJ/m²) averaged between 15°S-7°S in the Indian, and 6°S-12°N in the Pacific Ocean for a) REF, b) PAC and c) IND.

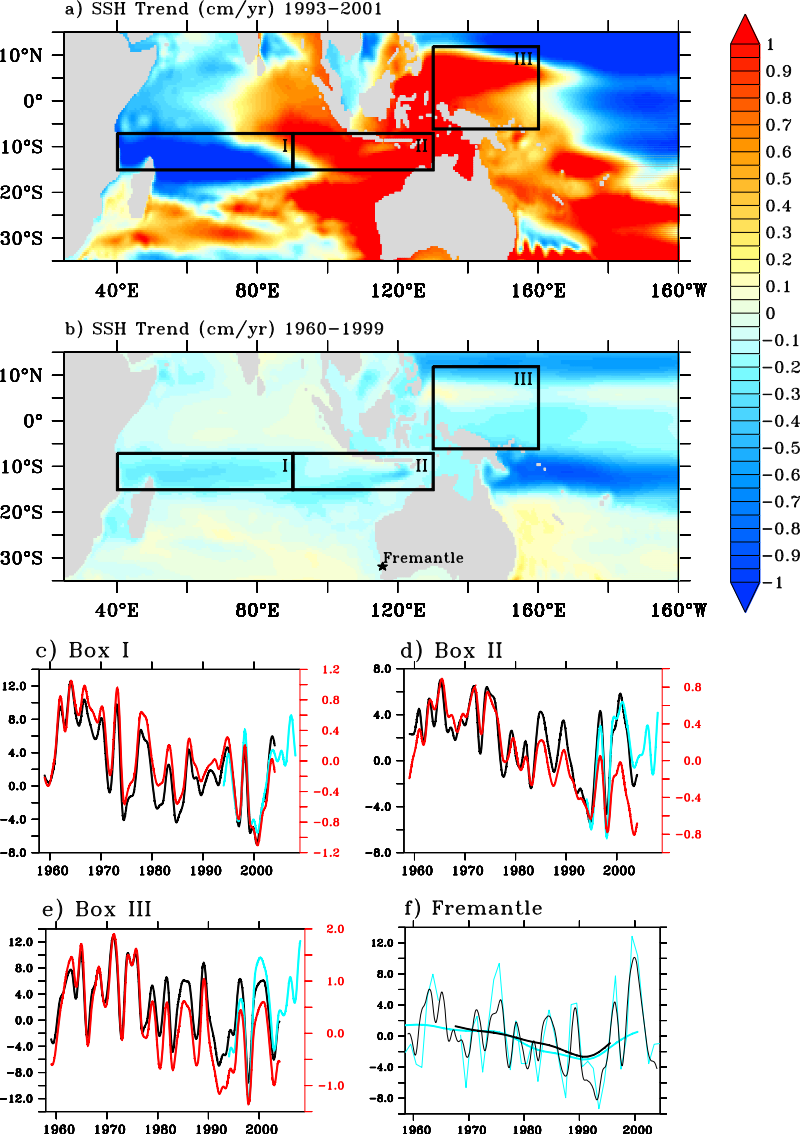
a) SSH Trend (cm/yr) 1993–2001
10°N
0°
10°S
20°S
30°S
40°E
80°E
120°E
160°E
160°W
I
II
III
1
0.9
0.8
0.7
0.6
0.5
0.4
0.3
0.2
0.1
0
−0.1
−0.2
−0.3
−0.4
−0.5
−0.6
−0.7
−0.8
−0.9
−1
b) SSH Trend (cm/yr) 1960–1999
Fremantle
c) Box I
d) Box II
e) Box III
f) Fremantle
1960
1970
1980
1990
2000

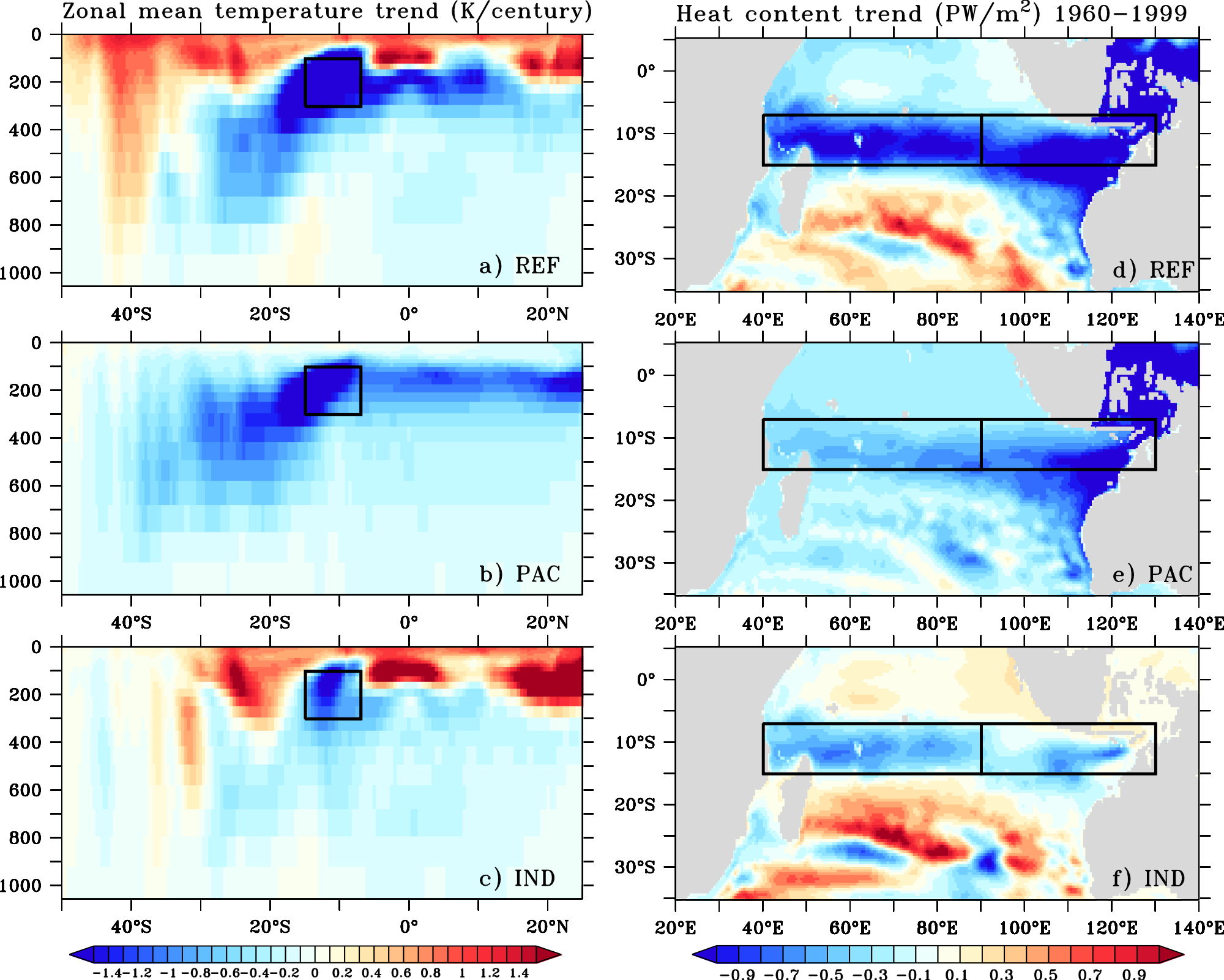
Zonal mean temperature trend (K/century)
Heat content trend (PW/m^2) 1960–1999
a) REF
b) PAC
c) IND
d) REF
e) PAC
f) IND
0
200
400
600
800
1000
40°S
20°S
0°
20°N
0°
10°S
20°S
30°S
20°E
40°E
60°E
80°E
100°E
120°E
140°E
−1.4 −1.2 −1 −0.8 −0.6 −0.4 −0.2 0 0.2 0.4 0.6 0.8 1 1.2 1.4
−0.9 −0.7 −0.5 −0.3 −0.1 0.1 0.3 0.5 0.7 0.9

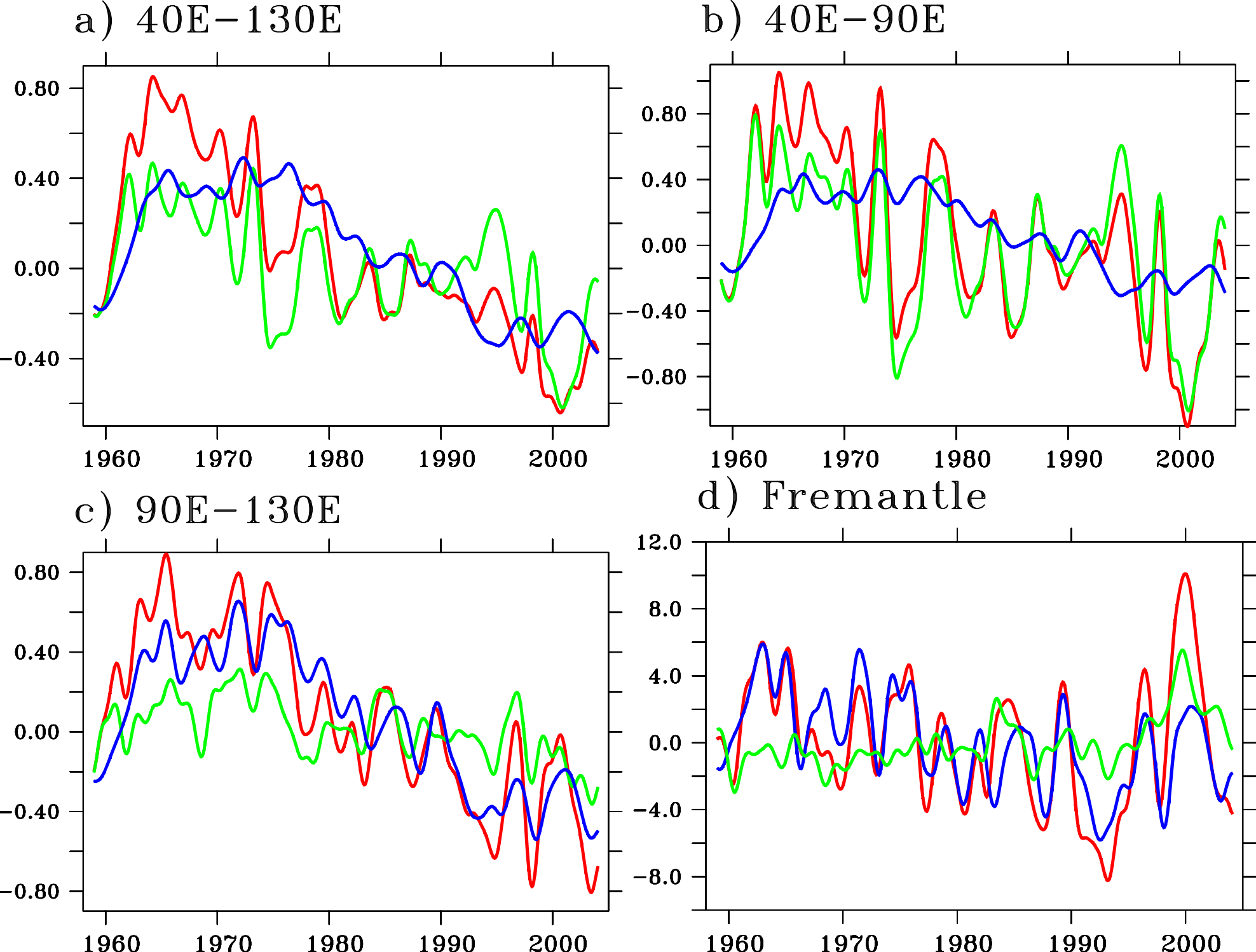
a) 40E−130E
b) 40E−90E
c) 90E−130E
d) Fremantle
0.80
0.40
0.00
−0.40
−0.80
12.0
8.0
4.0
0.0
−4.0
−8.0
1960
1970
1980
1990
2000

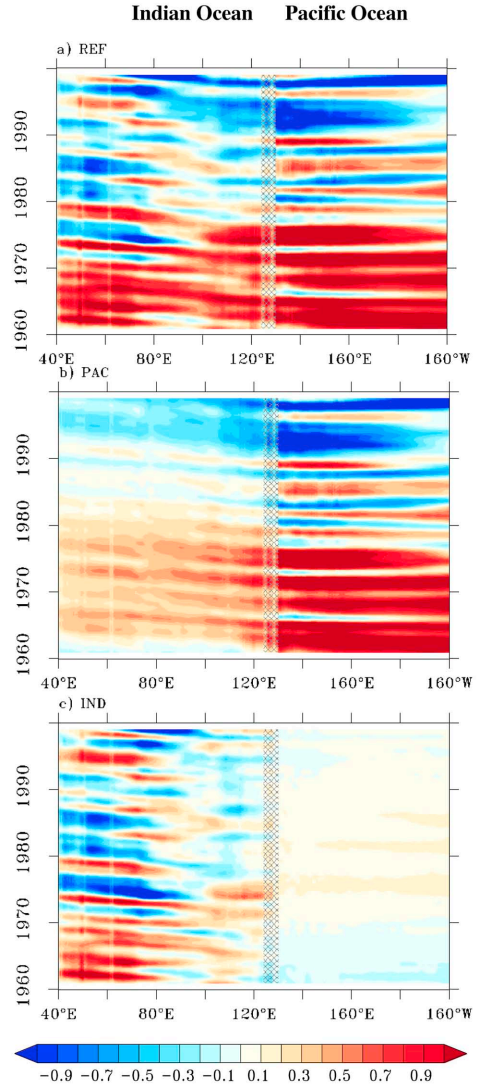
Indian Ocean
Pacific Ocean
a) REF
b) PAC
c) IND
1960
1970
1980
1990
40°E
80°E
120°E
160°E
160°W
−0.9 −0.7 −0.5 −0.3 −0.1 0.1 0.3 0.5 0.7 0.9